Influence of a strong magnetic field on the Wannier-Stark states of an electrically biased GaAs/$Al_xGa_{1-x}As$ superlattice

A. B. Hummel, T. Bauer, and H. G. Roskos
Physikalisches Institut der Johann Wolfgang Goethe-Universität, Robert-Mayer-Str. 2–4, D-60054 Frankfurt am Main, Germany

S. Glutsch
Institut für Festkörpertheorie und Theoretische Optik, Friedrich-Schiller-Universität Jena, Max-Wien-Platz 1, D-07743 Jena, Germany

K. Köhler
Fraunhofer-Institut für Angewandte Festkörperphysik, Tullastr. 72, D-79108 Freiburg, Germany
(Received 5 December 2001; revised manuscript received 8 May 2002; published 29 January 2003)

We present experimental and theoretical photocurrent spectra of a GaAs/AlGaAs superlattice under the influence of electric and magnetic fields parallel to the growth axis. In this field configuration, the charge carriers are subjected to zero-dimensional confinement. Depending on the fields, we observe a complicated interplay of Wannier-Stark and Landau levels. The experimental spectra are found to be in good agreement with numerical results.

DOI: 10.1103/PhysRevB.67.045319 PACS number(s): 73.21.Cd, 71.35.Ji, 71.70.Di, 71.70.Ej

I. INTRODUCTION

Since the first proposal of semiconductor superlattices by Esaki and Tsu,[1] artificial crystals have been investigated intensively as model structures for the coherent dynamics of electronic wave packets in a periodic potential. Application of a dc electric field parallel to the surface normal leads to the splitting of the superlattice minibands into Wannier-Stark ladders and finally produces quasi-two-dimensional confinement of charge carriers.[2–5] Simultaneous excitation of several Wannier-Stark states generates wave packets performing spatial oscillations, known as Bloch oscillations.[6–9] A thorough discussion of the physics of semiconductor superlattices is given in Ref. 10. More recent developments include spontaneous emission from Wannier-Stark ladders,[11] control of wave packets by ac and dc fields,[12] and the Zener breakdown in superlattices.[13]

In the last decade, much work has been done on the effects of an additional magnetic field on the optical[14–34] and transport[35–39] properties of semiconductor quantum wells and superlattices. A (sufficiently strong) magnetic field applied perpendicularly to the quantum-well layers (Faraday geometry) quantizes the motion of the carriers in the layer plane and reduces the dimensionality of the semiconductor. In this sense, a bulk semiconductor in a magnetic field is one dimensional, similar to a quantum wire,[40] and a quantum well in a perpendicular magnetic field can be considered as a zero-dimensional semiconductor, comparable to a quantum dot.[14] In the case of a superlattice, the confinement becomes intermediate between zero and one dimensions at sufficiently high field strengths, and the absorption spectrum is entirely discrete.[23,24,27,28] In a first approximation, assuming interaction-free electron-hole pairs, Wannier-Stark quantization and Landau quantization are independent of each other. The Coulomb interaction between electrons and holes leads to a complicated interference between Wannier-Stark and Landau quantizations, which is presently not fully understood. Besides the reduction of the dimensionality, the symmetry is reduced, and one observes a splitting of states with different magnetic quantum numbers.[20,21,26] If the magnetic field is applied parallel to the layers (Voigt geometry), strong mixing effects are expected,[24,25] and the structure of the spectrum is not understood at all.

In this paper, we present an experimental and theoretical analysis of the energy levels of a GaAs/$Al_{0.3}Ga_{0.7}As$ superlattice subjected to electric and magnetic fields parallel to the growth axis (Faraday geometry). We investigate the evolution of the spectrum with magnetic field and find a strong interference between Wannier-Stark and Landau levels. We achieve the closest agreement of experiment and theory one can obtain in the parabolic band model.

With respect to Ga(In)As/AlGa(In)As superlattices, prior experimental studies have focused on the following aspects: (i) the diamagnetic shift of transitions and their low-electric-field anticrossings,[33] (ii) the influence of fully zero-dimensional confinement on the interband transitions,[23] and (iii) the magnetic-field dependence of the lower Landau levels (Landau-level index $n \leqslant 3$) with respect to their spectral position[17,24,28] and oscillator strength.[28] Based on the classification suggested in Ref. 41, the superlattice structures investigated in the past were either short-period superlattices (with large miniband widths) (Refs. 17,23, and 24) or long-period superlattices (with small miniband width) (Refs. 28 and 33). Our structure, in contrast, is intermediate between these two regimes. The different quantum-well coupling strength allows us to observe features in our photocurrent spectra which could not be resolved or even were nonexistent in earlier experiments. The most important of these are (i) anticrossings between certain heavy-hole and light-hole magnetoexcitons, (ii) Landau fans with up to ten Landau levels at maximum magnetic field for both the spatially direct and the strongest spatially indirect Wannier-Stark transitions, and (iii) spin-split transitions (in photocurrent measurements with polarized light) exhibiting a very strong splitting for the $2s$-exciton transitions.

On the theoretical side, we point out that the treatment of Coulomb interactions and magnetic fields is numerically challenging already for ideal two-dimensional semiconduc-

tors.[14–16,18,20,22] For this reason, a number of theoretical papers on superlattices in a magnetic field applied in Faraday geometry handle only discrete spectra.[30,32,42] The Voigt geometry has been treated by Alexandrou *et al.*,[25] Dignam and Sipe,[43] and Young *et al.*,[30] mostly for limiting cases. The eigenvalue problem has been discussed for interaction-free particles.[19] Because of the large mathematical dimensionality of the eigenvalue problem, a simultaneous treatment of the Coulomb interaction and continuum states for a large range of parameters remains an open problem.

The numerical calculation of the optical absorption in superlattices is particularly difficult because of the three-dimensional nature of the problem. First high-resolution spectra of superlattices have been presented by Whittaker for an electric field alone (no magnetic field) and show a strong Fano effect in the line shape.[44] The Faraday geometry was treated by Barticevic *et al.*, but their numerical method is accurate only in the limit of large magnetic field.[32] Recently, a numerical method was developed based upon discretization in real space,[45] which allows one to efficiently calculate absorption spectra of complicated geometries with high resolution and should be able to treat the superlattice in Faraday geometry. For the Voigt geometry, no reliable theoretical spectrum has been published so far, and the problem is currently under investigation.[46]

The theoretical analysis presented in this paper utilizes the exact Kane functions instead of tight-binding approximations as in Ref. 32. Hence, our results fully converge and are reliable even in all limiting cases ($F=0$, $B=0$, no Coulomb interaction) and not only for large fields $B \geqslant 10$ T. The nonparabolicity of the energy bands is carefully taken into account and proves to be important for a quantitative analysis of the experimental data. The observation that the energy-dependent mass is independent of the electric field is important. Furthermore, we discuss why the effective exciton masses cannot be determined from the slope of particular exciton transitions subject to the magnetic field. A fan chart of the calculated data demonstrating the interference of Wannier-Stark and Landau quantizations is shown.

The paper is organized as follows. Section II starts with a description of the sample preparation and the experimental setup. Subsequently we give a detailed analysis of the experimental photocurrent spectra including a discussion of the Wannier-Stark ladder for $B=0$ and of measured angular momentum splittings. In Sec. III we give a review of the main theoretical aspects and show the calculated absorption spectra. In Sec. IV we summarize the major results of this study.

II. EXPERIMENT

A. Sample preparation and experimental setup

The superlattice investigated in this study was grown by molecular beam epitaxy on an n^+-doped GaAs substrate (doping density 10^{18} cm^{-3}). The undoped superlattice structure consists of 35 periods of 9.7-nm-thick GaAs wells and 1.7-nm-thick $Al_{0.3}Ga_{0.7}As$ barriers with 250- and 350-nm-thick undoped $Al_{0.3}Ga_{0.7}As$ buffer layers above and beneath the superlattice region, respectively. The growth direction is identical to the [001] crystallographic direction. The width of the first electron miniband is about 19 meV. An electric bias field can be applied between the doped GaAs substrate and a semitransparent Cr/Au Schottky contact (1 nm/5 nm) on top of the sample. A 200-nm-thick alloyed AuGe film serves as backside contact. The superlattice structure is the same as used for the observation of Bloch oscillations in Refs. 7 and 8 and for the investigation of the Coherent Hall Effect in Ref. 47.

The photocurrent spectra are measured with the unpolarized light of a 30-W halogen lamp propagating along the growth direction and spectrally dispersed by a 0.5-m monochromator with a grating of 1200 grooves/mm. The spectral resolution is better than 0.28 meV. Using a low-noise current-voltage converter followed by a lock-in amplifier we reach a signal-to-noise ratio of up to 500:1 peak to peak in case of zero bias voltage. Because of the rather large excitation spot (1.5 mm$\times$8 mm), broadening of the spectral features by residual spatial inhomogeneities of the superlattice parameters is possible, but seems not to be significant. For an excitation power of 35 nW, we estimate an electron-hole-pair density of 1.3×10^8 cm^{-3} (far below Mott density), if we assume a recombination time of 5 ns typical for bulk GaAs.[48] Under the influence of an electric field the recombination time should be much shorter. The sample is mounted in a magnet cryostat with a superconducting split-coil magnet providing magnetic fields up to 9 T and sample temperatures down to 4 K.

The electric field F, as function of the applied bias V_{ext}, is

$$F = \frac{-V_{\mathrm{ext}} - V_{\mathrm{int}}}{L} = F_{\mathrm{ext}} + F_{\mathrm{int}}, \tag{1}$$

where V_{int} is the built-in voltage of the Schottky diode, $F_{\mathrm{ext}} = -V_{\mathrm{ext}}/L$ and $F_{\mathrm{int}} = -V_{\mathrm{int}}/L$ are the external and intrinsic electric fields, and L is the total thickness of the intrinsic layer, which is 1.019 μm for the investigated sample structure. An applied voltage of $V_{\mathrm{ext}} = -V_{\mathrm{int}}$ corresponds to the flatband situation, where all Wannier-Stark states are degenerate. The built-in voltage depends not only on the pure sample structure, but also on the contact resistance of the backside metallization. Therefore different values of V_{int} for different pieces cut off from the same superlattice sample wafer are possible. The built-in voltage of the piece of the sample used for the experiments at zero magnetic field (from now on called sample 1) amounts to $V_{\mathrm{int}} = -0.55$ V, corresponding to an intrinsic electric field of about $F_{\mathrm{int}} = 5.5$ kV/cm. For the piece used for the experiments with an additional magnetic field (sample 2) we find $V_{\mathrm{int}} = -0.9$ V and $F_{\mathrm{int}} = 9$ kV/cm by comparing the data for $B=0$ for both sample 1 and sample 2. The backside metallization of sample 2 is ohmic as desired, sample 1 exhibits an additional voltage offset resulting from incomplete annealing.

B. Zero magnetic field: Wannier-Stark ladder

First, we study photocurrent spectra of sample 1 for zero magnetic field and different electric fields. The results are shown in Fig. 1.

Figure 1(a) shows photocurrent spectra for an electric bias V_{ext} ranging from $+0.3$ V to -1.1 V in steps of 0.05 V. By

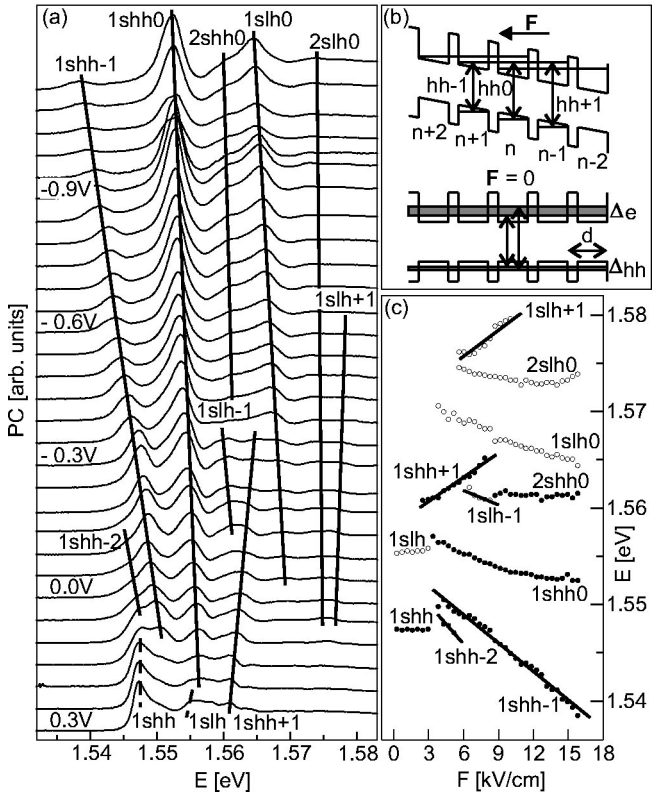

FIG. 1. (a) Measured photocurrent (PC) spectra of a GaAs/AlGaAs superlattice vs photon energy E for bias voltages from $+0.3$ V to -1.1 V corresponding to electric fields F from about 2.5 kV/cm to 16.7 kV/cm. The shift of the observed excitonic transitions with the electric field is indicated by straight lines. (b) Schematic drawing of the optical transitions in the superlattice for $F=0$ and $F\neq 0$. (c) Transition energies as function of the electric field.

comparison of spectra for positive and negative V_{ext}, the built-in voltage was found to be -0.55 V, corresponding to a built-in electric-field of $F_{\text{int}}=5.5$kV/cm. Thus the electric field range is $F=2.5$–16.7 kV/cm. The polarization of the light is linear, which is not relevant for $B=0$, because every transition is twofold degenerate.

The nomenclature of the observed excitonic miniband and Wannier-Stark transitions is as follows: hh and lh stand for electron–heavy-hole and electron–light-hole transitions, respectively; $1s$, $2s$, etc., represent the excitonic state, and the trailing number is the Wannier-Stark index l [cf. Fig. 1(b)].

The spectra for low electric fields ($V_{\text{ext}}=+0.3$–$+0.2$ V, $|F|=2.4$–3.4 kV/cm) are dominated by the $1s$ hh exciton of the first heavy-hole miniband at 1.5475 eV. At slightly higher energies we can identify the $1s$ lh exciton of the first light-hole miniband. The spectrum for $+0.15$ V bias ($F=4$ kV/cm) marks the transition from the miniband to the Wannier-Stark regime. With increasing electric field we observe the evolution of the $1s$ hh Wannier-Stark fan for $l=-2,-1,0,+1$ and of the $1s$ lh Wannier-Stark fan for $l=-1,0,+1$. In spite of their low oscillator strength we also observe higher exciton transitions: the $2s$ hh0 exciton flanking the $1s$ lh0 line and possibly the $2s$ lh0 exciton at 1.575 eV. The $1s$ hh0 and $1s$ lh0 lines show asymmetric absorption due to Fano coupling to the continua of lower Wannier-Stark transitions.[49]

Generally, one can distinguish between three different regimes: the miniband regime, where the energetic spacing of the Wannier-Stark Ladder is much smaller than the width of the minibands, a transition regime, where both energy scales are comparable, and the Wannier-Stark regime, where the Wannier-Stark-ladder spacing exceeds the miniband width. The transition regime is characterized by the coexistence of Franz-Keldysh and Wannier-Stark oscillations which leads to a complex interference pattern.[50]

In Fig. 1(c) the photocurrent peak energies are plotted versus electric field. In the miniband regime $|F|\rightarrow 0$, the positions of the excitons are nearly independent of the electric field. In the Wannier-Stark regime $|F|\rightarrow\infty$, we observe Wannier-Stark ladders, which originate not from the exciton positions at $F=0$, but from the center of the minibands. For moderate fields, as used in the experiment, the fan chart clearly shows deviations from a linear field dependence of the Wannier-Stark energies, especially of the $1s$ hh0 and $2s$ lh0 lines. This is because we observe excitonic, not single-particle, transitions: at higher electric fields the exciton binding energies of the Wannier-Stark transitions with index $l=0$ increase sublinearly with increasing field and approach a constant.[41] The effect is much smaller for transitions with $l\neq 0$, because the Coulomb interaction is smaller for spatially indirect excitons.[44,51] There is no continuous transition between the miniband regime and Wannier-Stark regime because of an infinite number of level crossings for small fields.

C. Nonzero magnetic field: Evolution of Landau fans

In order to investigate the influence of an additional magnetic field on the superlattice energy states we measured photocurrent spectra of sample 2 for several external bias fields. As mentioned above, the built-in voltage of this sample was found to be -0.9 V, corresponding to a built-in electric field of $F_{\text{int}}=9$ kV/cm. Figure 2 shows the evolution of the spectrum with magnetic field for fixed electric field $F=9$ kV/cm (a) and $F=12$ kV/cm (b). The magnetic field ranges from 0 to 9 T and the polarization of the light is linear.

Figure 2(a) shows photocurrent spectra at zero external bias. In this case, the electric field is equal to the intrinsic field, $F=F_{\text{int}}=9$ kV/cm. We reach a very good signal-to-noise ratio of about 500:1 peak to peak. Therefore even small photocurrent maxima represent real transitions. By comparing to the spectra at zero magnetic field [Fig. 1(a)] the peaks that are indicated in the spectrum for $B=0$ T can be assigned to certain Wannier-Stark transitions. Figure 2(a) nicely shows the evolution of the Landau fan of the ns hh0 magnetoexcitons ($n\geqslant 1$) up to the $10s$ hh0 transition: with increasing magnetic field the transitions shift to higher energies while separating from each other. The observation of a magnetoexcitonic Landau fan is in agreement with similar experiments of Alexandrou *et al.* done on an undoped $GaAs/Al_{0.35}Ga_{0.65}As$ superlattice.[24]

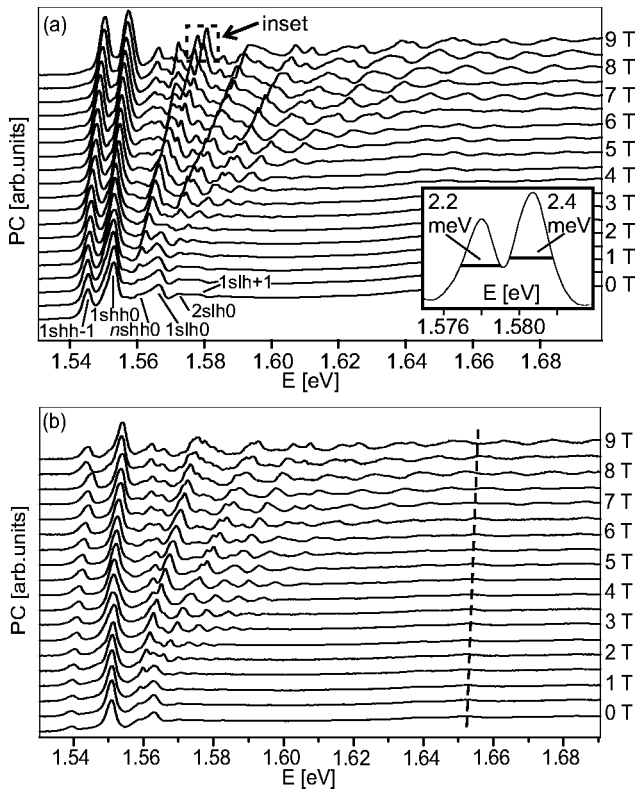

FIG. 2. Measured photocurrent (PC) spectra vs photon energy E for magnetic fields B from 0 T to 9 T and electric fields of 9 kV/cm (a) and 12 kV/cm (b). The dashed line indicates the $1s$ hh0 transition of the (2,2) subband. Inset of (a): fit of the experimental line shapes to Lorentzians.

In the limit of high magnetic fields the energies of a Landau fan should behave as[18,30]

$$E_{nl}(B) = E_l + \left(n + \frac{1}{2}\right)\hbar\frac{eB}{m_\parallel} + O(B^{1/2}), \tag{2}$$

where E_l is the continuum edge of the lth Wannier-Stark transition and n is the Landau quantum number. A quantitative criterion for the high-field limit is that the cyclotron energy $\hbar eB/m_\parallel$ be much larger than the Rydberg energy of the exciton. Assuming a reduced cyclotron mass $m_\parallel = 0.06$, this is the case for $B \gg 2.4$ T. Furthermore, there should be two Landau fans for each Wannier-Stark transition, stemming from the heavy-hole and light-hole band, and band-mixing effects are expected in the intermediate-field region. For small magnetic fields clear deviations from the linear behavior emerge.[30] In particular, in the limit $B \to 0$, the excitons show a diamagnetic shift quadratic in B.

There is also a strong interaction of Wannier-Stark and Landau ladders on the account of Coulomb interaction. This interaction is particularly strong when the quantization energies are of the same order of magnitude. With $F = 9$ kV/cm and $a = 11.4$ nm, the Wannier-Stark energy $e|F|a$ amounts to about 10 meV, which equals the cyclotron energy $\hbar e|B|/m_\parallel$ for electrons at $B = 5.2$ T. We shall discuss the interference of Wannier-Stark and Landau ladders in detail in the next section, where we also make a comparison with results of a numerical calculation.

Results for $F = 12$ kV/cm are shown in Fig. 2(b). This time, because $V_{\text{ext}} \neq 0$, a permanent dark current reduces the signal-to-noise ratio and fewer details can be observed. Because of the larger electric field, the exciton belonging to the vertical Wannier-Stark transition ($l = 0$) is more strongly confined, its binding energy is larger, and the region of B, for which the shift is diamagnetic, should be larger, compared to the case $F = 9$ kV/cm. This is actually verified in the experimental spectra: for $F = 12$ kV/cm the transition from diamagnetic to linear behavior takes place roughly at 4 T, for $F = 9$ kV/cm at 2 T. Otherwise, the qualitative behavior of the spectrum as function of the magnetic field is the same as observed in Fig. 2(a).

The determination of effective exciton masses from the spectra is difficult mainly for the following reason: because of their diamagnetic shift for small values of B, the slope of the $1s$-exciton energies cannot be used to determine the corresponding effective mass; higher excitons, however, cannot be identified unambiguously over the whole magnetic-field range.

In Figs. 3(a) and 3(b) we try a detailed analysis of the transitions for 9 kV/cm and 12 kV/cm, respectively, in the energy range between 1.538 eV and 1.590 eV, where the spectra contain a number of well-resolved features.

The spectrum at zero magnetic field in Fig. 3(a) is dominated by the $1s$ hh-1, $1s$ hh0, and $1s$ lh0 transitions; moreover, one can identify the ns hh0 ($n > 1$), $1s$ hh-2, $2s$ lh0, and $1s$ lh$+1$ features. With increasing magnetic field both the $1s$ hh-1 and the $1s$ hh0 transitions slightly shift to higher energies, while their energetic spacing decreases from 7.3 meV at 0 T to 6.8 meV at 9 T. Because of its smaller exciton binding energy, the $1s$ hh-1 transition is influenced more strongly by the magnetic field so that its magnetic-field-induced blueshift is stronger than that of the $1s$ hh0 line.

In two-dimensional semiconductors, in the limit $B \to \infty$, the oscillator strengths of the excitons increase linearly with magnetic field. However, especially for the $1s$ exciton with a small spatial extension, this limit is reached only for extremely large fields.[14] Generally, for low and intermediate magnetic fields, the oscillator strength should increase more rapidly with field for excitons with a large spatial extension, such as higher-order ($2s$, $3s$, ...) or spatially indirect ($l \neq 0$) excitons. Indeed, for the $1s$ hh-1 we observe an increase of the oscillator strength by a factor of 1.9, compared to 1.1 for the $1s$ hh0 transition. Further examples are the $1s$ hh$+1$ and $2s$ hh0 transitions: both can hardly be identified at 0 T, but with increasing magnetic field distinct peaks emerge.

As expected, we observe several transitions belonging to Landau fans of Wannier-Stark states other than the transitions with the index $l = 0$. We can identify the $1s$ and $2s$ magnetoexcitons of the heavy-hole Wannier-Stark transitions with indices -1, 0, and $+1$, the $1s$ hh-2 transition and the $1s$ lh magnetoexcitons with Wannier-Stark indices -2, -1, 0, and $+1$. There is good agreement between the en-

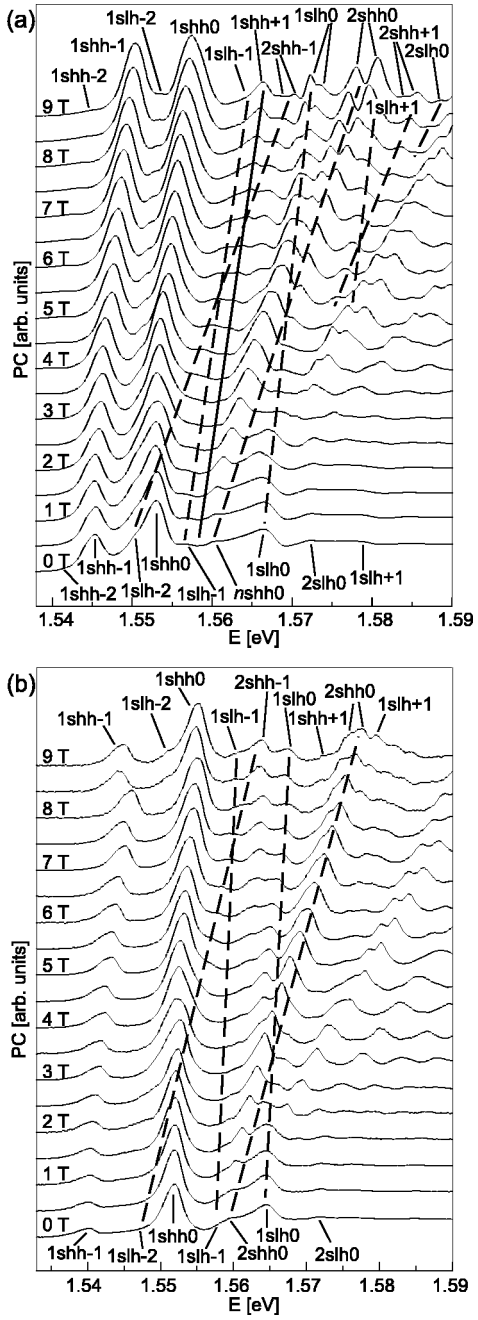

FIG. 3. Detailed analysis of the observed transitions for an electric field of $F=9$ kV/cm (a) and $F=12$ kV/cm (b). Dashed lines indicate anticrossings of states.

ergy spacing of neighboring $2s$ hh excitons and of the corresponding $1s$ hh excitons, corroborating the correctness of the above assignment.

The valence-band coupling leads to anticrossings of heavy-hole and light-hole states. Besides the anticrossing of the fundamental light-hole transition $1s$ lh0 with the $2s$ hh0 state at a magnetic field around 4.5 T as a preeminent example, we observe anticrossings of the $1s$ lh-1 with the $2s$ hh-1 and of the $1s$ lh$+1$ with the $2s$ hh$+1$ transition. Because the experiments are carried out with linearly polarized light, we observe a spin splitting of the $2s$ hh0 state in the spectra at high magnetic fields, as discussed in detail at the end of this section.

Though the photocurrent spectra for $F=12$ kV/cm in Fig. 3(b) are a little bit more noisy than those for $F_{\mathrm{int}}=9$ kV/cm due to the increased current flow, real transitions are well distinguished from features caused by noise. The spectra for $B=8.5$ T and $B=9.0$ T show a larger energy spacing between the $1s$ hh-1 and $1s$ hh0 transition compared to the spectra at lower magnetic field. This suggests that those two spectra correspond to a slightly higher electric field, the reason for which is unknown. At zero magnetic field we observe the same transitions as in Fig. 3(a), except for the $1s$ lh$+1$ and $1s$ hh-2 features. Because of the stronger electric bias field, interwell transitions have lost oscillator strength. As B increases from 0 to 9T, the oscillator strength of the $1s$ hh0 transition increases by a factor of about 1.1. At the same time, the oscillator strength of the $1s$ hh-1 exciton even increases by a factor of 2.8. This might be explained by the dependence of the excitonic binding energies of the Wannier-Stark transitions on the electric bias field: with increasing electric field, the binding energy of the transitions with the index $l=0$ increases, whereas for $l=-1$ it slightly decreases.[41] In the spectra for high magnetic fields we can identify the $1s$ and $2s$ magnetoexcitons of the heavy-hole Wannier-Stark transitions with indices -1 and 0, the $1s$ hh$+1$ magnetoexciton and $1s$ lh excitons with indices -2, -1, 0, and $+1$. As indicated in the figure, only the very pronounced anticrossing of the $1s$ lh0 with the $2s$ hh0 transition at a magnetic field around 4 T and that of the $1s$ lh-1 with the $2s$ hh-1 transition are resolved in the photocurrent spectra. Further anticrossings of weak transitions above the $2s$ hh0 peak cannot be assigned to particular magnetoexciton states.

D. Spin splitting

The experimental photocurrent spectra (Figs. 2 and 3), taken with linearly polarized light, contain features caused by a spin splitting of states in the magnetic field. First, we observe a slight broadening of both the $1s$ hh0 and $1s$ hh-1 transition with increasing magnetic field. Second, the ns hh0 magnetoexcitons ($n>1$) split into double-peak features each with a small linewidth. This is quite in contrast to the experimental results of Alexandrou *et al.* who observe a line broadening only.[24] Especially for $F=9$ kV/cm the double peaks are very well resolved. As shown in the inset of Fig. 2(a), the $2s$ hh0 states have linewidths of about 2.2 meV and 2.4 meV.

In semiconductor heterostructures, in the presence of quantum confinement, the Γ_8 valence band ($j=3/2$) splits into a heavy-hole band ($m_j=\pm 3/2$) and a light-hole band ($m_j=\pm 1/2$). A magnetic field applied in the growth ([001]) direction leads to Zeeman splitting of the heavy-hole, light-hole, and conduction band with $m_j=+3/2,-3/2$, $m_j=+1/2,-1/2$, and $m_s=+1/2,-1/2$, respectively. Then the absorption (photocurrent, photoluminescence excitation) spectra for σ^+ (right circular) and σ^- (left circular) polarization are different. The situation is shown schematically in Fig. 4(a). The Landé factor of the electron is negative because of the strong spin-orbit coupling.[52] Due to the Coulomb inter-

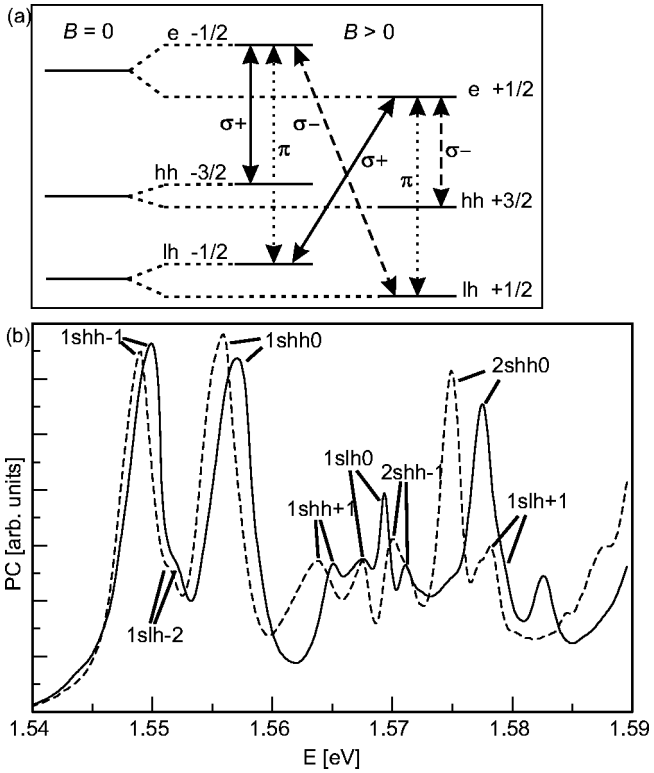

FIG. 4. (a) Schematic representation of the energy states of superlattice electrons and holes in an external magnetic field and allowed optical dipole transitions at excitation with σ^+, σ^-, and π polarized light. (b) Photocurrent (PC) spectra vs photon energy E in Faraday geometry at a magnetic field of 8 T and an intrinsic electric field of about 9 kV/cm for σ^+ (solid line) and σ^- (dashed line) circularly polarized excitation light.

action between electron, heavy hole, and light hole, the situation is far more complicated than in the single-particle picture, shown in Fig. 4(a), and magnetoexciton spectra are generally very sensitive to the details of the band structure.

In order to visualize the spin splitting, we repeat the measurement with polarized light. The photocurrent spectra are shown in Fig. 4(b) for an intrinsic electric field of $F=9$ kV/cm and a magnetic field $B=8$ T measured with σ^+ and σ^- circularly polarized excitation light. The spectra evidence that the broadening of the main heavy-hole transitions and the doublet structure of the higher ns hh0 magnetoexcitons are consequences of a spin splitting of these states. The splitting energy amounts to 1.0 meV for the $1s$ hh−1, 1.2 meV for the $1s$ hh0, and 2.5 meV for the $2s$ hh0 transition, which corresponds to measured and calculated splitting energies obtained for uncoupled[26] and coupled[21] quantum wells as far as they can be resolved. The splitting is stronger for $2s$ excitons than for the corresponding $1s$ excitons, probably due to the stronger Coulomb interaction of the excitonic ground state. Higher excitons ($3s$, $4s$, etc.) cannot be identified unambiguously in the spectra, but the spin splitting is not expected to increase linearly with the excitonic state n according to experimental observations for uncoupled quantum wells.[26] Whether the spin splitting is stronger for the heavy-hole than for the light-hole states cannot be answered confidently because $2s$ light-hole transitions cannot be identified in the spectra.

III. THEORY

A. Single-particle properties

The confinement of electron (e) and hole (h) is modeled by the periodic potentials

$$U_{e,h}(z)=\begin{cases}0 & \text{for} \quad 0\leqslant z<a-b,\\ H_{e,h} & \text{for} \quad a-b\leqslant z<a,\end{cases}$$

$$U_{e,h}(z)=U_{e,h}(z+a), \tag{3}$$

where a is the superlattice period, b is the barrier thickness, and $H_{e,h}$ are the band discontinuities. The motion of the individual particles in an electric field F in the growth direction is governed by the Schrödinger equation

$$\left[-\frac{\hbar^2}{2m_{e,h\perp}}\frac{d^2}{dz^2}+U_{e,h}(z)\pm eFz\right]\psi_{e,hl}(z)=E_{e,hl}\psi_{e,hl}(z). \tag{4}$$

A set of eigenvalues with the property $E_{e,hl}=E_{e,h0}\pm eFal$ and $\psi_{e,hl}(z)=\psi_{e,h0}(z-na)$ with l integer is called a Wannier-Stark ladder. Strictly speaking, the spectrum is continuous and the eigenfunctions are not square integrable.[53] For field strengths well below the Zener breakdown, the eigenfunctions which correspond to below-barrier minibands are strongly localized and can be approximated by Kane functions.[2]

The Γ_1 conduction band of GaAs is strictly parabolic in the limit of small Bloch wave vectors $\mathbf{k}$. For larger values of $\mathbf{k}$, the symmetry will only be cubic. The expansion up to fourth order in $\mathbf{k}$, neglecting spin splitting, is[54]

$$E_e(\mathbf{k})=\frac{\hbar^2k^2}{2m_e}+\alpha_0k^4+\beta_0(k_y^2k_z^2+k_z^2k_x^2+k_x^2k_y^2)+\cdots. \tag{5}$$

To approximate the above expression by a parabolic dispersion, we follow the procedure of Ref. 55. We neglect the nonparabolicity of the perpendicular motion and set $m_{e\perp}=m_e$. For the in-plane motion, we average over the angle $\arg(k_x+ik_y)$ and take the expectation value over the eigenfunctions of the perpendicular motion. Then the in-plane dispersion becomes

$$E_{e\parallel}(\mathbf{k}_\parallel)=\frac{\hbar^2k^2}{2m_{e\parallel}}, \tag{6}$$

where

$$m_{e\parallel}=\frac{m_e}{1+\dfrac{2m_e}{\hbar^2}(2\alpha_0+\beta_0)\langle k_z^2\rangle} \tag{7}$$

is known as the energy-dependent effective mass. The increase of the parallel mass affects both the exciton binding energy[55] and the energies of the Landau levels.[56] In the Kane approximation, the expectation value

$$\langle k_z^2\rangle=\int_{-\infty}^{+\infty}dz\left|\frac{d}{dz}\psi_{el}(z)\right|^2 \tag{8}$$

is independent of the electric field, as can be shown from the analytic properties of the Kane functions.[57] For a quantitative

study, the correct in-plane electron mass (7) is more important than the details of the valence-band dispersion, because the electron mass is much smaller than the hole mass.

The effective masses for the heavy and light holes in the growth ([001]) direction, expressed by the Luttinger parameters, are $m_{\mathrm{hh}\perp}=m_0/(\gamma_1-2\gamma_2)$ and $m_{\mathrm{lh}\perp}=m_0/(\gamma_1+2\gamma_2)$. The in-plane dispersion of the valence band is generally complicated. It is written by several authors that the in-plane hole masses are $m_{\mathrm{hh}\|}=m_0/(\gamma_1+\gamma_2)$ and $m_{\mathrm{lh}\|}=m_0/(\gamma_1-\gamma_2)$, known as mass reversal. However, these values are correct only under the assumptions of perfect confinement (infinite barriers, zero thickness) and in the limit $k_\|\to 0$. The first assumption is never fulfilled. For example, $m_{\mathrm{lh}\|}$ can be negative (see, e.g., Fig. 24 of Ref. 58). Furthermore, the extension of the nth eigenfunction in $k_\|$ space is in the order of $\sqrt{n}/\lambda_{\mathrm{mag}}$, where $\lambda_{\mathrm{mag}}=(\hbar/eB)^{1/2}$ is the magnetic length. For example, for $B=5$ T, the extension of the fifth eigenfunction in $k_\|$ space is of the order of 2×10^7 cm^{-1} (about 6 times the length of the abscissa in Fig. 24 of Ref. 58). Therefore, we are in the limit of *large* $k_\|$. The Landau levels of heavy and light holes in the limit of large Landau quantum numbers are described by the cyclotron masses m_{hhc} and m_{lhc} for $\mathbf{B}\|[001]$, which have a complicated dependence on the Luttinger parameters.[59] We shall use this approximation for the lowest (hh) miniband. In order to accurately treat the light hole, one would need to take into account the whole Luttinger Hamiltonian. We neglect them in our calculations. As shown in the comparison with the experiment this is justified because they play only a minor role.

B. Optical absorption

The optical absorption is related to the eigenvalue problem of an electron-hole pair, subjected to Coulomb interaction and quantum confinement. In the absence of electron-hole pairs, the Coulomb interaction is screened by a static dielectric constant ε, which takes into account the electronic background and the ionic lattice. We assume a magnetic field in the growth direction (Faraday geometry). Taking into account the symmetry of the problem, we have to solve the eigenvalue problem

$$\hat{H}\Phi_\Lambda(\rho,Z,z)=E_\Lambda\Phi_\Lambda(\rho,Z,z), \tag{9}$$

with the differential operator

$$\hat{H}=-\frac{\hbar^2}{2m_\|}\frac{1}{\rho}\frac{\partial}{\partial\rho}\left(\rho\frac{\partial}{\partial\rho}\right)-\frac{\hbar^2}{2m_{e\perp}}\frac{\partial^2}{\partial z_e^2}-\frac{\hbar^2}{2m_{h\perp}}\frac{\partial^2}{\partial z_h^2}+U_e(z_e)$$
$$+U_h(z_h)-\frac{e^2}{4\pi\varepsilon_0\varepsilon\sqrt{\rho^2+z^2}}+eFz+\frac{e^2B^2}{8m_\|}\rho^2.$$

$$\frac{1}{m_\|}=\frac{1}{m_{e\|}}+\frac{1}{m_{h\|}} \tag{10}$$

and the boundary condition

$$\Phi_\Lambda(\rho,Z,z)=\Phi_\Lambda(\rho,Z+a,z). \tag{11}$$

Here ρ is the in-plane distance and $Z=\lambda z_e+(1-\lambda)z_h$ and $z=z_e-z_h$ are the center and relative coordinates of the perpendicular motion. For the numerical solution by finite differencing it is useful to set $\lambda=0$ or $\lambda=1$ so that the mesh points for the electron and hole coordinates z_e, z_h are identical.

For numerical reasons, we introduce a (large) finite domain for the coordinates ρ and z with vanishing boundary conditions. With the normalization of the eigenfunctions,

$$\int_{-L/2}^{+L/2}dz\int_{-a/2}^{+a/2}dZ\int_0^R d\rho 2\pi\rho\Phi_\Lambda^*(\rho,Z,z)\Phi_{\Lambda'}(\rho,Z,z)$$
$$=\delta_{\Lambda\Lambda'}, \tag{12}$$

the optical absorption is given by

$$\alpha(\omega)\propto\frac{1}{a}\sum_\Lambda\left|\int_0^a dZ\Phi_\Lambda(0,Z,0)\right|^2$$
$$\times\frac{\hbar\epsilon}{(E_\Lambda+E_g-\hbar\omega)^2+(\hbar\epsilon)^2}, \tag{13}$$

where E_g is the band gap of the active layer and $\hbar\epsilon$ is the homogeneous broadening, which is taken as a constant.

The eigenvalue problem (9)–(11) cannot be solved directly. Instead, we determine the absorption coefficient (13) by the equation-of-motion method.[45]

An alternative to the solution in real space is the expansion into Kane or Wannier functions and the solution of a set of ordinary differential equations. This is the standard method so far and has been used by several authors.[32,43,41,44,51] The numerical effort is significantly smaller, but the calculation is limited to a finite number of subband pairs (mostly one) and Zener tunneling is neglected. We shall compare both methods: the calculation in real space and the expansion into Wannier functions. The matrix elements of the exciton Hamiltonian in the basis of Wannier functions are given in Ref. 13.

The material parameters for GaAs are $m_e=0.067m_0$, $m_{h\perp}=m_{\mathrm{hh}\perp}=0.377m_0$, $\alpha_0=-213.2$ meV nm^4, $\beta_0=-249.3$ meV nm^4,[54] $m_{h\|}=m_{\mathrm{hhc}}=0.491m_0$,[59] $\varepsilon=13.1$, and $E_g=1.52$ meV. The band discontinuities between GaAs and $Al_xGa_{1-x}As$ as functions of the Al molar fraction x are $H_e=790x$ meV and $H_h=460x$ meV.[60] For the samples described in Sec. II we have $x=0.3$, $a=11.4$ nm, and $b=1.7$ nm. For the homogeneous broadening we assume $\hbar\epsilon=1$ meV.

C. Numerical results

Figure 5 shows theoretical spectra of the superlattice under consideration for magnetic fields in the range of $B=0$–9 T and two different electric fields $F=9$ kV/cm (a) and $F=12$ kV/cm (b). The spectra are calculated using discretization in real space so that, in principle, all subbands are taken into account. The only transition associated with higher subbands, which can be seen in the spectrum, is the (2,2) transition, which is marked by a dashed line. Its relative oscillator strength is very small, and for this miniband pair

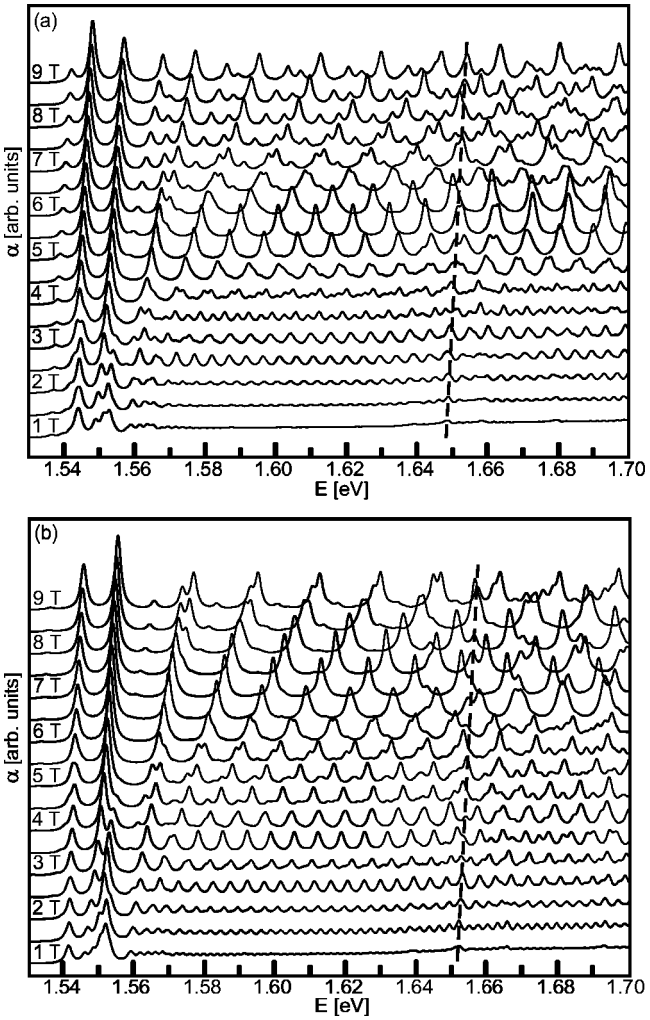

FIG. 5. Theoretical absorption spectra of the investigated superlattice structure in Faraday geometry for magnetic fields B from 1 T to 9 T and for an electric field $F=9$ kV/cm (a) and for $F=12$ kV/cm (b). Dashed lines indicate the main second-miniband electron–heavy-hole Wannier-Stark transition.

no Wannier-Stark transitions other than $l=0$ are observed, in agreement with the experiment as likewise indicated by a dashed line in Fig. 2(b). Also, the broadening of the lines due to tunneling is negligible. This suggests that a projection onto the Wannier functions of the first electron and hole miniband should also produce accurate results, which was found to be true by comparison of the numerical results. The energy-dependent mass for the first electron miniband was found to be $m_{e\|}=0.0704m_0$, which is about 5% larger than m_e. With this correction and the hh cyclotron mass, we were able to reproduce the experimental cyclotron energy for the hh with an error of about 3%. It is worthwhile to note that a correct electron mass is more important than the details of the hole dispersion. An error of 5% for the electron mass has the same consequences as an error of 35% for the mass of the heavy hole.

Let us now point out the differences between theory and experiment, which are related to the two-band model. As the light-hole transitions are neglected in the theory the theoretical spectra show about half as many transitions as the experimental ones. Due to the assumption of a constant and rather small homogeneous broadening in the calculations, distinct resonances can be observed in the whole energy range. In contrast, in the experiment the line broadening increases with energy and the Landau fans are seen only for large values of B when the cyclotron energy exceeds the homogeneous broadening.

The theoretical spectra evidence the existence of separate Landau fans for spatially direct and spatially indirect heavy-hole Wannier-Stark transitions. As observed experimentally, the Landau fan assigned to the spatially direct Wannier-Stark transitions is very pronounced whereas the Landau fans for the spatially indirect Wannier-Stark transitions are much weaker. In the energy range from 1.53 eV to 1.70 eV we can identify the Landau fan of the ns hh0 magnetoexcitons ($n\geqslant 1$) up to the $9s$ hh0 transition. Between these strong features smaller peaks are resolved which belong to the ns hh-1 and ns hh$+1$ Landau fans. The peaks right below individual ns hh0 transitions [most pronounced in Fig. 5(a)] can be identified by their magnetic-field dependence as the $(n-1)s$ hh$+1$ transitions. In the same way we identify the small peaks just above the ns hh0 transitions as the $(n+1)s$ hh-1 states. In Fig. 5(b) the spatially indirect transitions are even smaller than in Fig. 5(a) because of the stronger electric field, which leads to stronger charge carrier confinement in individual quantum wells. This is also observed in the experimental photocurrent spectra for $F=12$ kV/cm [cf. Figs. 2(b) and 3(b)]. The $10s$ hh0 exciton lies beyond the plotted energy range because neighboring ns hh0 transitions are separated by about 17 meV instead of about 15 meV in the experimental spectra. Starting from energies of about 1.65 eV we find features belonging to higher subbands both in the theoretical and in the experimental spectra. The strongest of these features (indicated by dashed lines in Fig. 5) can be assigned to the $1s$ hh0 transition of the second miniband.

Finally, we make a comparison between measured and calculated fan charts. In Fig. 6, the derivative of the photocurrent (or absorption) $d\alpha(\omega)/d\omega$ is plotted as function of the photon energy E (x axis) and the magnetic field B (y axis). The electric field is fixed at $F=9$ kV/cm. Experimental results (a) are compared with the result of a numerical calculation (b). The theoretical spectra were obtained using Wannier functions as base functions, which is much less computationally intensive than the solution entirely in real space. For this reason, miniband transitions other than (1,1) are absent in the calculated fan chart.

We observe good qualitative and, in part, quantitative agreement between experiment and theory. In contrast to the individual spectra (Figs. 2 and 5), this representation allows us to better observe the evolution of the peaks with magnetic field. One can clearly observe the diamagnetic shift of the lowest Landau levels ($n=0$) and the nearly linear shift of the excited Landau levels ($n>0$). The differentiated spectra reveal a number of anticrossings between Landau levels from different Wannier-Stark transitions. Especially in the theoretical fan chart, we observe interference patterns when $\hbar\omega_c/eFa=p/q$ with p and q being small primes. In the

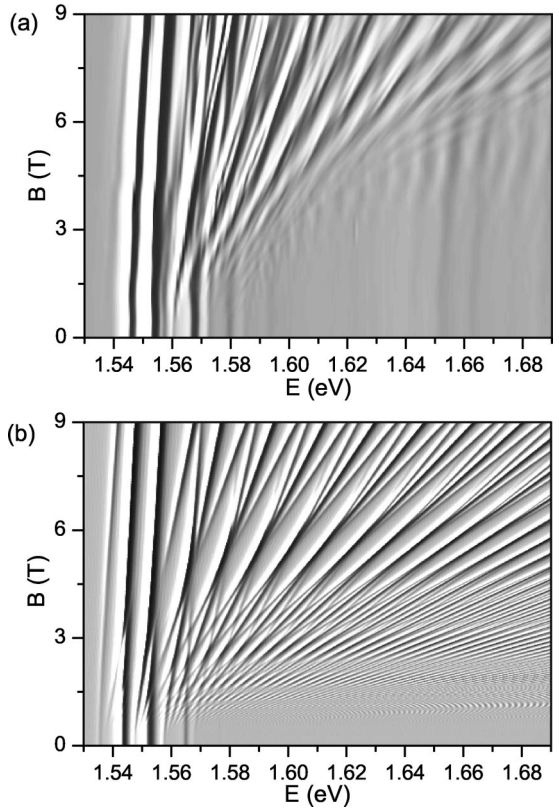

FIG. 6. Comparison between experimental (a) and theoretical (b) fan chart. Gray-scale plot of the differentiated photocurrent (absorption) as a function of the photon energy E and the magnetic field B.

experiment, these patterns are visible only in part, because as a consequence of the line broadening, higher Landau levels are resolved only for large magnetic fields. Another important observation is that the light-hole transitions play a minor role and there are hardly any features in the experimental fan chart, which are absent in theory. Therefore, a more realistic theoretical approach is to neglect the light hole, rather than perform separate calculations for heavy and light holes, which tends to overestimate the light-hole transitions.

IV. CONCLUSIONS

In summary we investigated the influence of a magnetic field on the energy levels of a GaAs/AlGaAs superlattice electrically biased along the growth axis. With increasing magnetic field applied parallel to the electric field the excitonic states of each Wannier-Stark level separate and shift to higher energies forming so-called Landau fans. For certain values of the magnetic field anticrossings of states occur. The photocurrent spectra show a coupling between the $1s$ lh$l$ and $2s$ hh$l$ transitions. The magnetic field also leads to an increase of the oscillator strength which is much stronger for the spatially indirect than for the spatially direct Wannier-Stark transitions. Therefore, Bloch oscillations as a result of quantum interferences of spatially direct with spatially indirect transitions should be difficult to observe. Photocurrent measurements with circularly polarized excitation light evidence a spin splitting of states for high magnetic fields. The main features, observed in the experiment, can be explained with good qualitative agreement by theoretical calculations based upon a two-band model. The absorption-photocurrent spectra exhibit complicated patterns which are a consequence of the interference between Wannier-Stark and Landau quantization.

ACKNOWLEDGMENTS

We gratefully acknowledge numerous discussions with L. Bányai, G. Meinert, and H. Haug (Universität Frankfurt). We are indebted to W. G. Schmidt for useful comments on the manuscript. This work has been supported by the Schwerpunktprogramm ''Quantenkoh'árenz in Halbleitern'' of the Deutsche Forschungsgemeinschaft. We acknowledge computing time from the John von Neumann-Institut für Computing, Forschungszentrum Jülich.

[1] L. Esaki and R. Tsu, IBM J. Res. Dev. **14**, 61 (1970).
[2] E. O. Kane, J. Phys. Chem. Solids **12**, 181 (1959).
[3] J. Bleuse, G. Bastard, and P. Voisin, Phys. Rev. Lett. **60**, 220 (1988).
[4] E. E. Mendez, F. Agulló-Rueda, and J. M. Hong, Phys. Rev. Lett. **60**, 2426 (1988).
[5] E. E. Mendez and G. Bastard, Phys. Today **46** (6), 34 (1993).
[6] J. Feldmann, K. Leo, J. Shah, D. A. B. Miller, J. E. Cunningham, T. Meier, G. von Plessen, A. Schulze, P. Thomas, and S. Schmitt-Rink, Phys. Rev. B **46**, 7252 (1992).
[7] C. Waschke, H. G. Roskos, R. Schwedler K. Leo, H. Kurz, and K. Köhler, Phys. Rev. Lett. **70**, 3319 (1993).
[8] R. Martini, G. Klose, H. G. Roskos, H. Kurz, H. T. Grahn, and R. Hey, Phys. Rev. B **54**, 14 325 (1996).
[9] P. Haring Bolivar, F. Wolter, A. Müller, H. G. Roskos, H. Kurz, and K. Köhler, Phys. Rev. Lett. **78**, 2232 (1997).
[10] H. T. Grahn, *Semiconductor Superlattices* (World Scientific, Singapore, 1995).
[11] G. Scamarcio, F. Capasso, A. L. Hutchison, D. L. Sivico, and A. Y. Cho, Phys. Rev. B **57**, 6811 (1998); R. Colombelli, A. Straub, F. Capasso, C. Gmachl, M. I. Blakey, A. M. Sergent, S. N. G. Chu, K. W. West, and L. N. Pfeiffer, J. Appl. Phys. **91**, 3526 (2002).
[12] R.-B. Liu and B. Zhu, J. Phys.: Condens. Matter **12**, L741 (2000).
[13] S. Glutsch, F. Bechstedt, B. Rosam, and K. Leo, Phys. Rev. B **63**, 085307 (2001).
[14] J. B. Stark, W. H. Knox, D. S. Chemla, W. Schäfer, S. Schmitt-Rink, and C. Stafford, Phys. Rev. Lett. **65**, 3033 (1990).
[15] O. Akimoto and H. Hasegawa, J. Phys. Soc. Jpn. **22**, 181 (1967).
[16] M. Shinada and K. Tanaka, J. Phys. Soc. Jpn. **29**, 1258 (1970).
[17] G. Belle, J. C. Maan, and G. Weimann, Solid State Commun. **56**, 65 (1985).
[18] A. H. MacDonald and D. S. Ritchie, Phys. Rev. B **33**, 8336 (1986).

[19] J. C. Maan, in *Physics and Applications of Quantum Wells and Superlattices*, Vol. 170 of *Proceedings NATO Advanced Study Institute, Series B: Physics*, edited by E. E. Mendez and K. von Klitzing (Plenum, New York, 1987); Surf. Sci. **196**, 518 (1988).
[20] G. E. W. Bauer and T. Ando, Phys. Rev. B **37**, 3130 (1988).
[21] H. Chu and Y.-C. Chang, Phys. Rev. B **40**, 5497 (1989).
[22] J. L. Zhu, Y. Cheng, and J. J. Xiong, Phys. Rev. B **41**, 10 792 (1990).
[23] B. Soucail, P. Voisin, M. Voos, and M. Allovon, Surf. Sci. **229**, 468 (1990); R. Ferreira, B. Soucail, P. Voisin, and G. Bastard, Phys. Rev. B **42**, 11 404 (1990).
[24] A. Alexandrou, E. E. Mendez, and J. M. Hong, Phys. Rev. B **44**, 1934 (1991).
[25] A. Alexandrou, M. M. Dignam, E. E. Mendez, J. E. Sipe, and J. M. Hong, Phys. Rev. B **44**, 13 124 (1991).
[26] S. Schmitt-Rink, J. B. Stark, W. H. Know, D. S. Chemla, and W. Schäfer, Appl. Phys. A: Solids Surf. **53**, 491 (1991).
[27] Z. Barticevic, M. Pacheco, and F. Claro, Surf. Sci. **267**, 545 (1992).
[28] A. Roth, E. Lugagne-Delpon, and P. Voisin, Can. J. Phys. **70**, 819 (1992).
[29] O. Kühn, N. J. M. Horing, and R. Enderlein, Semicond. Sci. Technol. **8**, 513 (1993).
[30] P. M. Young, H. Ehrenreich, P. M. Hui, and N. F. Johnson, J. Appl. Phys. **74**, 7369 (1993).
[31] B. S. Monozon, A. G. Zhilich, J. L. Dunn, and C. A. Bates, J. Phys.: Condens. Matter **6**, 4009 (1994).
[32] Z. Barticevic, M. Pachecho, and F. Claro, Phys. Rev. B **51**, 14 414 (1995).
[33] H. Kümmel, R. Till, and A. Philipp, Phys. Rev. B **60**, 4470 (1999).
[34] M. Pacheco and Z. Barticevic, Phys. Rev. B **64**, 033406 (2001).
[35] W. Müller, H. T. Grahn, K. von Klitzing, and K. Ploog, Phys. Rev. B **48**, 11 176 (1993).
[36] L. Canali, F. Beltram, M. Lazzarino, and L. Sorba, Superlattices Microstruct. **22**, 155 (1996).
[37] A. C. Goldberg, J. R. Anderson, J. W. Little, and W. A. Beck, Physica B **216**, 372 (1996).
[38] P. Kleinert and V. V. Bryksin, Phys. Rev. B **56**, 15 827 (1997); V. V. Bryksin and P. Kleinert, Physica B **269**, 163 (1999).
[39] F. Q. Yan and X. L. Lei, J. Phys.: Condens. Matter **13**, 6625 (2001).
[40] S. Glutsch, U. Siegner, M.-A. Mycek, and D. C. Chemla, Phys. Rev. B **50**, 17 009 (1994).
[41] M. M. Dignam and J. E. Sipe, Phys. Rev. B **43**, 4097 (1991).
[42] M. Pacheco, Z. Barticevic,and F. Claro, Phys. Rev. B **46**, 15 200 (1992).
[43] M. M. Dignam and J. E. Sipe, Phys. Rev. B **45**, 6819 (1992).
[44] D. M. Whittaker, Europhys. Lett. **31**, 55 (1995).
[45] S. Glutsch, D. S. Chemla, and F. Bechstedt, Phys. Rev. B **54**, 11 592 (1996).
[46] S. M. Stepanow *et al.* (unpublished).
[47] T. Bauer, J. Kolb, A. B. Hummel, H. G. Roskos, Y. Kosevich, and K. Köhler, Phys. Rev. Lett. **88**, 086 801 (2002).
[48] A. Dargys and J. Kundrotas, *Handbook on Physical Properties of Ge Si GaAs and InP* (Science and Encyclopedia, Vilnius, 1994).
[49] C. B. Holfeld, F. Löser, M. Sudzius, K. Leo, D. M. Whittaker, and K. Köhler, Phys. Rev. Lett. **81**, 874 (1998).
[50] K. H. Schmidt, N. Linder, G. H. Döhler, H. T. Grahn, K. Ploog, and H. Schneider, Phys. Rev. Lett. **72**, 2769 (1994).
[51] N. Linder, Phys. Rev. B **55**, 13 664 (1997).
[52] M. Oestreich and W. W. Rühle, Phys. Rev. Lett. **74**, 2315 (1995).
[53] J. E. Avron, J. Zak, A. Grossmann, and L. Gunther, J. Math. Phys. **18**, 918 (1977).
[54] U. Rössler, Solid State Commun. **49**, 943 (1984).
[55] L. C. Andreani and A. Pasquarello, Phys. Rev. B **42**, 8928 (1990).
[56] U. Ekenberg, Phys. Rev. B **40**, 7714 (1989).
[57] S. Glutsch, J. Phys.: Condens. Matter **11**, 5533 (1999).
[58] G. Bastard, *Wave Mechanics Applied to Semiconductor Heterostructures* (Les Editions de Physique, Les Ulis, 1992).
[59] U. Rössler, Solid State Commun. **65**, 1279 (1988).
[60] S. Adachi, *GaAs and Related Materials* (World Scientific, Singapore, 1994).